LIMNOLOGY AND OCEANOGRAPHY
Letters

ASLO
Open Access

*Limnology and Oceanography Letters* 7, 2022, 427–434

doi: 10.1002/lol2.10270

LETTER

# In situ estimates of net primary production in the open-ocean Gulf of Mexico

*Bo Yang* [1,2a]* *Fabian Gomez* [2,3] *Claudia Schmid*,[2] *Molly Baringer*[2]

[1]Cooperative Institute for Marine and Atmospheric Studies, Rosenstiel School of Marine and Atmospheric Science, University of Miami, Miami, Florida; [2]Atlantic Oceanographic and Meteorological Laboratory (AOML), Miami, Florida; [3]Northern Gulf Institute, Mississippi State University, Starkville, Mississippi

## *Scientific Significance Statement*

Net primary production (NPP), defined as gross photosynthetic carbon fixation minus the organic carbon respired by the phytoplankton communities, is a key metric of marine biological carbon production. Most NPP studies in the Gulf of Mexico (GoM) focused on coastal and shelf areas, and a limited number of studies on the open-ocean GOM were based on satellite observations and could not provide direct information at depth. Float-based bio-optical data were available in the open-ocean GoM, but lacked concurrent field calibrations. In this work, the float bio-optical data were adjusted against the satellite products, and used to obtain the first year-round depth-resolved NPP estimates in this area. The results showed distinct seasonal patterns in surface and depth-integrated NPP, and revealed that the major controls of NPP in the surface and subsurface layers were nutrient supply and light level, respectively.

## *Abstract*

Net primary production (NPP) measurements in the open-ocean Gulf of Mexico are scarce and mostly limited to satellite-derived surface estimates. Profiling floats can obtain depth-resolved chlorophyll (Chl) and backscattering (bbp) data for NPP estimates, but historical float data in this region lacked field calibrations. We adjusted the float data with satellite Chl, generating a consistent dataset for deriving the first year-round depth-resolved NPP estimates in this region. The results revealed distinct seasonal patterns in surface NPP and depth-integrated (0–100 m) total NPP, with the peak values in the winter and summer, respectively. The results showed that for most of the year subsurface (20–100 m) contributes

*Correspondence: bxy189@miami.edu

[a]Present address: Department of Marine Biology and Ecology, Rosenstiel School of Marine and Atmospheric Science, University of Miami, Miami, Florida, USA

**Associate editor:** Sarah Fawcett

**Author Contributions Statement:** B.Y. designed the experiments and analyzed the data. F.G. provided the dissolved inorganic nitrogen climatology from model simulation. B.Y. prepared the manuscript with contributions from all co-authors.

**Data Availability Statement:** The float data can be obtained at https://www.ncei.noaa.gov/archive/accession/0159562 (Hamilton and Leidos 2017). Satellite-derived Chl, bbp, and PAR are from http://sites.science.oregonstate.edu/ocean.productivity/1080.by.2160.8day.inputData.php. The processed data used in this manuscript are available in the Zenodo repository https://doi.org/10.5281/zenodo.5544582.

Additional Supporting Information may be found in the online version of this article.

more to the total (0–100 m) NPP than the surface layer (0–20 m), and the major controls of NPP in these two layers were light level and nutrient supply, respectively.

Biological production of organic carbon by phytoplankton communities is central to the carbon cycle and marine ecosystems. Net primary production (NPP), defined as gross photosynthetic carbon fixation minus the organic carbon respired by phytoplankton communities, is a key metric of marine biological carbon production. The Gulf of Mexico (GoM) provides habitat for fish and other marine organisms and is of great social, economic and ecological importance for this area (Muller-Karger et al. 2015, Davis 2017). Most NPP studies in the GoM focused on coastal and shelf regions, especially the areas influenced by the Mississippi–Atchafalaya River System (e.g., Zhao and Quigg 2015). A limited number of NPP studies were conducted in the open-ocean GoM, mostly based on satellite observations (e.g., Muller-Karger et al. 2015), which could not provide direct information at depth. Field measurements of depth-resolved NPP in the open-ocean GoM are scarce and limited to a certain season (e.g., Stukel et al. 2021, Yingling et al. 2021). Recent model studies (e.g., Gomez et al. 2018, Damien et al. 2021, Kelly et al. 2021) suggested that vertical mixing, lateral advection, and other mesoscale activities (e.g., Loop Current eddies) play important roles in the seasonal variability of biological carbon production in the oligotrophic open-ocean GoM.

The development of autonomous platforms (e.g., underwater glider, profiling float) makes it possible to obtain depth-resolved bio-optical parameters for NPP estimates. For example, year-round depth-resolved NPP estimates have been derived for the western North Atlantic, using field-calibrated chlorophyll (Chl) and backscattering (bbp) data from profiling floats (Yang et al. 2021). From 2011 to 2015, eight profiling floats with Chl and bbp sensors were deployed by the Bureau of Ocean Energy Management (BOEM) in the GoM for a Lagrangian analysis of deep ocean circulation (Green et al. 2014). Although there was a lack of concurrent shipboard measurements for field calibration, the work by Pasqueron de Fommervault et al. (2017) showed that it is feasible to adjust the float measurements with satellite products. Although the satellite product may not be the "gold standard" and the absolute values of the adjusted Chl may still be off, this approach provides a "consistent" dataset for analyzing the spatiotemporal patterns of Chl in the open-ocean GoM (Pasqueron de Fommervault et al. 2017).

In this study, we evaluated Chl and bbp data from BOEM floats against the satellite remote sensing products, and generated a consistent dataset that can be used to derive depth-resolved NPP in the open-ocean GoM. The spatial (vertical) and temporal (seasonal) variations of NPP and possible mechanisms behind such distribution patterns were analyzed. This study also served as a pilot study of the recently-launched Biogeochemical Argo profiling float (BGC-Argo) program in the GoM funded by the National Oceanic and Atmospheric Administration.

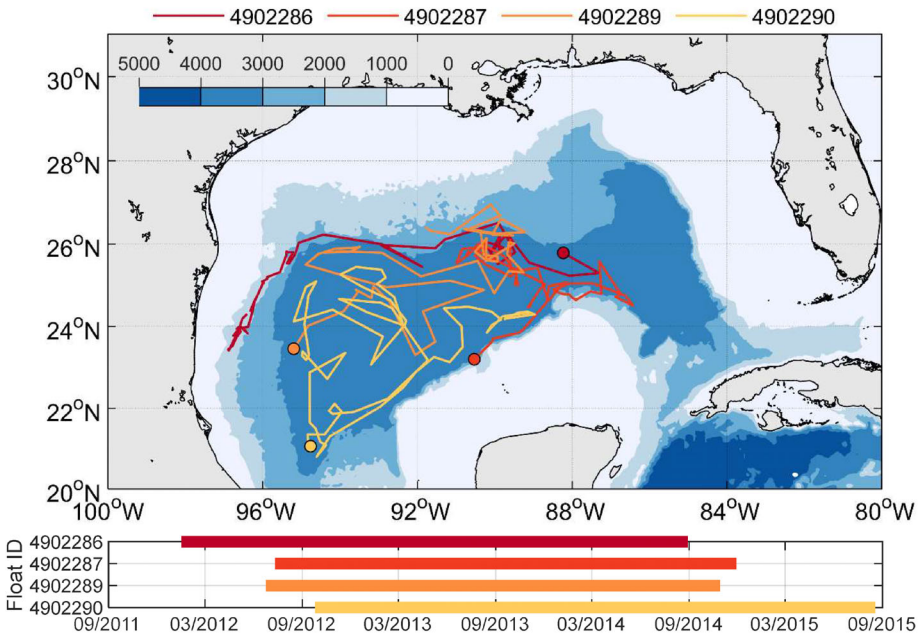


**Fig. 1.** Trajectories of four profiling floats with the initial float deployment locations denoted by filled circles. The background color indicates bottom depth (m). The float deployment durations are presented in the bar chart.

## Methods

### Study area and data acquisition

This study utilized the bio-optical data (Chl and bbp) from four profiling floats deployed by BOEM from 2012 to 2015 in the open-ocean GoM (bottom depth between 1500 and 4000 m, Fig. 1). These floats measured pressure, temperature, salinity, Chl, and bbp from the ocean surface to 1500 m depth, with a temporal resolution of 14 days (Green et al. 2014, Pasqueron de Fommervault et al. 2017). A total of 237 profiles were used for this study, roughly covering a transitional region (Damien et al. 2018) between the Loop Current-dominated southern GoM and the Mississippi–Atchafalaya River-dominated northern GoM. Mixed layer depth (MLD) was calculated from density profiles (derived from temperature and salinity measured by the profiling floats), using a density criterion (depth with a density difference larger than 0.1 kg $m^{-3}$ relative to the density at 10 m, Stukel et al. 2021).

Satellite-based estimates of surface Chl, bbp, and surface photosynthetically active radiation ($PAR_{surf}$) came from Moderate Resolution Imaging Spectroradiometer (MODIS) products, with a spatial resolution of 0.167 by 0.167° and a temporal resolution of 8 days (http://sites.science.oregonstate.edu/ocean.productivity/1080.by.2160.8day.inputData.php). The dissolved inorganic nitrogen (DIN; including nitrate and ammonium) profiles were used to help discussing the NPP distribution patterns, because the biological carbon production in the oligotrophic regions is based on both nitrate (new production) and ammonium (regenerated production) (Selph et al. 2021, Yingling et al. 2021). Since the BOEM floats were not equipped with nutrient sensors, we used the model outputs (monthly climatology from 2012 to 2014) from GoMBio (Gomez et al. 2018), a biogeochemical model based on the Regional Ocean Model System, with a horizontal resolution of 8 km and 37 sigma-coordinate (bathymetry-following) vertical levels. A one-dimension interpolation in time was first applied to the satellite and model data, to match the time of each float profile, and then a two-dimension interpolation in space was applied to interpolate the gridded satellite data and model outputs to the exact float location.

### Float data adjustment

The float-measured Chl and bbp at the shallowest sampling depth (~ 8 m) were first evaluated against the sea surface satellite estimates (Fig. S1). Although the float-measured surface bbp and satellite-based surface bbp were of the same magnitude, no significant linear relationship was found between them (Fig. S1a–d). As a result, to avoid any potential artifacts, no adjustment was applied to the float bbp data. On the other hand, good linear relationship between the float-measured surface Chl and satellite-derived surface Chl was found for all four floats (Fig. S1e–h), with correlation coefficient ($R$) between 0.65 to 0.76 and root mean standard deviation (RMSD) between 0.08 to 0.17 mg $m^{-3}$ (Table 1). Therefore, the linear regression results shown in Table 1 were used to adjust the float Chl profiles.

### NPP calculation

The carbon-based productivity model (CbPM; Behrenfeld et al. 2005, Westberry et al. 2008) was used to calculate the depth-resolved NPP. The CbPM model was chosen because: (1) CbPM-based satellite global NPP product has been widely used, and is available for direct comparison; (2) Yang et al. (2021) showed that the float-based NPP estimates with CbPM had a good agreement with the NPP estimated from the state-of-the-art $^{14}C$ incubation method.

NPP was calculated as the product of phytoplankton carbon ($C_{phyto}$, mg C $m^{-3}$) and phytoplankton specific growth rate ($\mu$, $day^{-1}$).

$$\mathrm{NPP} = C_{phyto} \times \mu \,\mathrm{mg\,C\,m^{-3}\,day^{-1}}. \quad (1)$$

$C_{phyto}$ was calculated using the relationship between $C_{phyto}$ and bbp at 470 nm (Graff et al. 2015).

$$C_{phyto} = 12128 \times bbp_{470} + 0.59\,\mathrm{mg\,C\,m^{-3}}. \quad (2)$$

Therefore, the float-measured bbp at 700 nm ($bbp_{700}$) was first converted to $bbp_{470}$ using Eq. 3 (Boss et al. 2013, Boss and Haëntjens 2016).

$$bbp_{470} = bbp_{700} \times \left(\frac{470}{700}\right)^{-0.78}\,\mathrm{m^{-1}}. \quad (3)$$

$\mu$ was calculated using the updated CbPM (Westberry et al. 2008).

$$\mu = \frac{2 \cdot \mathrm{Chl}/C_{phyto} \cdot \left(1 - \exp^{-5I_z}\right)}{0.022 + (0.045 - 0.022) \cdot \exp^{-3I_z}}\,\mathrm{day^{-1}}, \quad (4)$$

where Chl is the chlorophyll concentration (mg $m^{-3}$), and $I_z$ is the daily mean light level at each depth (mol photons $m^{-2}$ $day^{-1}$). $I_z$ was estimated using satellite-derived surface photosynthetically active radiation at the ocean surface ($PAR_{surf}$):

$$I_z = \mathrm{PAR_{surf}} \times \exp\left(-K_{PAR} \times Z\right)\,\mathrm{mol\,photon\,m^{-2}\,day^{-1}}, \quad (5)$$

where $Z$ is the depth, and $K_{PAR}$ is the diffuse attenuation coefficient of PAR, calculated using Eqs. 6a and 6b from Morel et al. (2007).

$$K_{PAR} = 0.0864 + 0.884 \times K_{490} - 0.00137 \times K_{490}^{-1}, \text{when MLD} \le K_{490}^{-1}\,\mathrm{m^{-1}}, \quad (6a)$$

$$K_{PAR} = 0.0665 + 0.874 \times K_{490} - 0.00121 \times K_{490}^{-1}, \text{when MLD} > K_{490}^{-1}\,\mathrm{m^{-1}} \quad (6b)$$

where $K_{490}$ is the 490 nm diffuse attenuation coefficient ($m^{-1}$), calculated from float-measured chlorophyll $a$ concentration (Morel and Maritorena 2001):

**Table 1.** The results from type II linear regression used to adjust the float chlorophyll (Chl) values with satellite data.

| | Chl (float) = a × Chl (satellite) + b | | | |
|---|---|---|---|---|
| **Float ID** | **4902286** | **4902287** | **4902289** | **4902290** |
| a | 4.14 ± 0.53 | 3.12 ± 0.38 | 3.05 ± 0.35 | 4.94 ± 0.69 |
| b | −0.33 ± 0.07 | −0.20 ± 0.04 | −0.17 ± 0.04 | −0.38 ± 0.08 |
| R | 0.71 | 0.74 | 0.76 | 0.65 |
| RMSD | 0.17 | 0.08 | 0.10 | 0.13 |

a: Slope; b: Intersect; R: correlation coefficient; RMSD: root mean standard deviation.

$$k_{490} = 0.0166 + 0.07242 \times \mathrm{Chl}^{0.68955}\ \mathrm{m}^{-1}. \quad (7)$$

Monthly climatologies were created to analyze the seasonal variations of depth-resolved NPP, by averaging all the NPP estimates from each month (January–December). There were 17 to 22 NPP profiles for each month, with float locations spreading relatively evenly in the study area (Fig. S2).

## *Results and discussion*

### Comparison of surface NPP derived from satellite and profiling float

A total of 237 individual surface NPP estimates were used to evaluate the performance of float-derived NPP. The adjusted float data yielded surface NPP values close to the satellite estimates (Fig. 2a), with a slope of linear regression = 0.68 ± 0.04, intercept = 3.16 ± 0.46, $R$ = 0.71, and RMSD = 2.22 mg m$^{-3}$. The linear regression result of the monthly NPP climatologies showed a slope of 0.62 ± 0.07 and an intercept of 3.70 ± 0.68, with $R$ of 0.94 and RMSD = 0.57 mg m$^{-3}$ (Fig. 2b), indicating that the float-derived NPP was suitable for analyzing the seasonal variation of NPP (Fig. 2c).

### Seasonal variations of surface and depth-integrated NPP

The monthly climatologies of MLD (from float measurements) and surface PAR (PAR$_{surf}$, from satellite) are presented in Fig. 3a. MLD was between 10 m (June) to 60 m (January), and PAR$_{surf}$ was between 1 mol photon m$^{-2}$ h$^{-1}$ (December) to 2.3 mol photon m$^{-2}$ h$^{-1}$ (May). The seasonal pattern of surface NPP followed the seasonal variations of surface nitrate concentration (Fig. 3b), with high NPP (~ 14 mg m$^{-3}$ day$^{-1}$) in the winter and low values in the summer (~ 8 mg m$^{-3}$ day$^{-1}$), consistent

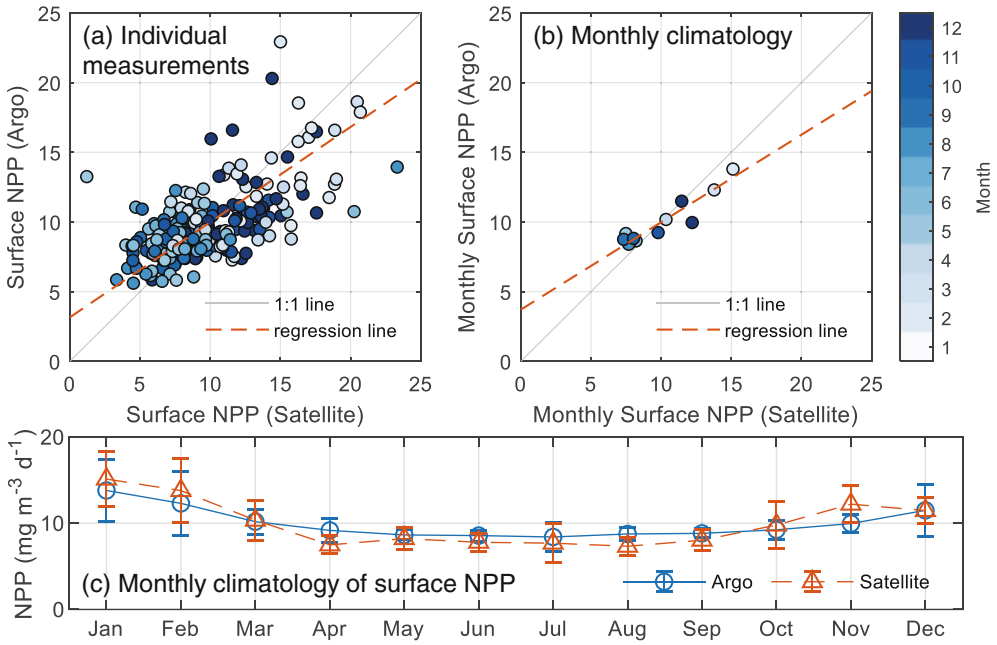


**Fig. 2.** Comparisons of float and satellite-derived surface NPP (unit: mg m$^{-3}$ day$^{-1}$). (**a**) Float NPP against satellite NPP ($n$ = 237); (**b**) float NPP against satellite NPP (monthly climatology); (**c**) monthly climatology of surface NPP created from individual float and satellite measurements, the error bars indicate the 50% quantile of monthly mean NPP. The gray solid line and red dash line in panels (**a**) and (**b**) indicate 1 : 1 line and type II linear regression line, respectively.

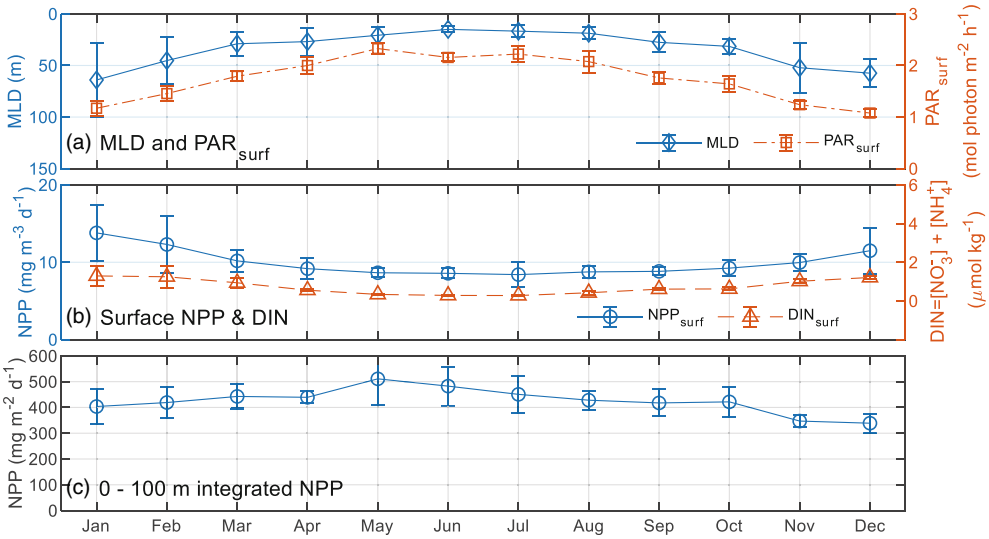


**Fig. 3.** (**a**) Monthly climatologies of mixed layer depth (MLD, m) and surface photosynthetically active radiation ($PAR_{surf}$, mol photon $m^{-2}$ $h^{-1}$); (**b**) monthly climatologies of surface net primary production (mg $m^{-3}$ $day^{-1}$) derived from float data and surface DIN (nitrate + ammonium) concentration ($\mu$mol $kg^{-1}$) from model output; (**c**) monthly climatologies of 0–100 m integrated NPP (mg $m^{-2}$ $day^{-1}$) derived from float data. Error bars indicate the 50% quantile of the data used to compute the monthly climatology.

with the seasonal pattern reported by former studies using satellite-based observations (Muller-Karger et al. 2015) and numerical models (Gomez et al. 2018). This pattern was consistent with the seasonality of MLD, with high surface NPP when MLD was deep and low surface NPP when MLD was shallow (Fig. 3a,b), indicating that the winter high surface NPP was most likely due to the increased surface nitrate concentration from deep mixing, and the low surface nitrate concentration in the stratified shallow summer mixed layer lead to low surface NPP. The other factor that might play a role in summer low surface NPP is photoacclimation: in the summer when the surface light level is too strong the phytoplankton cells reduce the concentration of light-harvesting pigments (e.g., Chl) to protect themselves, which leads to low Chl and low NPP in the surface.

Compared with the surface NPP, depth-integrated NPP is a better index for the phytoplankton carbon production in the water column. As shown in Fig. 3c, the 0–100 m depth-integrated total NPP increased from 400 mg $m^{-2}$ $day^{-1}$ in January to a maximum of over 500 mg $m^{-2}$ $day^{-1}$ in May, then continued decreasing to the lowest value of 340 mg $m^{-2}$ $day^{-1}$ in December. Such seasonal variation is entirely different from the seasonal pattern of surface NPP, which indicates the importance of obtaining depth-resolved NPP data for the studies of marine carbon production. The highest 0–100 m integrated NPP was observed in May. Although the float-based 0–100 m integrated NPP (510 mg $m^{-2}$ $day^{-1}$, equivalent to ~ 42 mmol $m^{-2}$ $day^{-1}$) was higher than the estimates (24–29 mmol $m^{-2}$ $day^{-1}$) from the April–May 2017/2018 in situ experiments conducted in the region to the northeast of our research area (Stukel et al. 2021, Yingling et al. 2021), the shapes of depth profile were similar (Fig. 4a in this work vs. Fig. 2 in Stukel et al. 2021). Possible explanations for the difference in the absolute NPP value includes the spatial/temporal mismatch of these two studies (Fig. S2), and the lack of shipboard field calibrations for the profiling float data.

For the oligotrophic subtropical ocean, nutrient supply is a key factor that controls the biological carbon production. On the other hand, the light availability is the major control of the vertical distribution of NPP. Therefore, for the analysis of depth-resolved NPP, we present the results in terms of monthly climatologies of float NPP (Fig. 4a,b), modeled DIN (Fig. 4c), and photosynthetically active radiation derived from float and satellite data (PAR, Fig. 4d).

From January to May, the NPP in the upper 20 m of the water column gradually decreased (Fig. 4a,b) due to the decreasing DIN (Fig. 4c). Meanwhile, DIN in the deeper layer (20–100 m) was still relatively abundant (Fig. 4c) and the light condition continued to improve from January to May (Fig. 4d, increased PAR and deepened $Z_{1\%}$). As a result, NPP in 20–100 m of the water column significantly increased (Fig. 4a,b), which led to continuous increase in 0–100 m depth-integrated total NPP (Fig. 3c). After May, the light level at depth started to decline (Fig. 4d), the NPP in the 20–100 m of water column started to decrease (Fig. 4a,b). Meanwhile, DIN in the upper 20 m of water column started to increase in June, as the deepening MLD brought more nutrients to the near surface (Fig. 4c). Because the decrease of deeper layer (20–100 m) NPP was more significant than the increase of 0–20 m NPP (Fig. 4b), the 0–100 m depth-integrated NPP decreased (Fig. 3c). Overall, from March to October the 20–100 m layer produced more NPP than the 0–20 m layer; for February and November the contributions from those two layers were equally important; and in December and January the

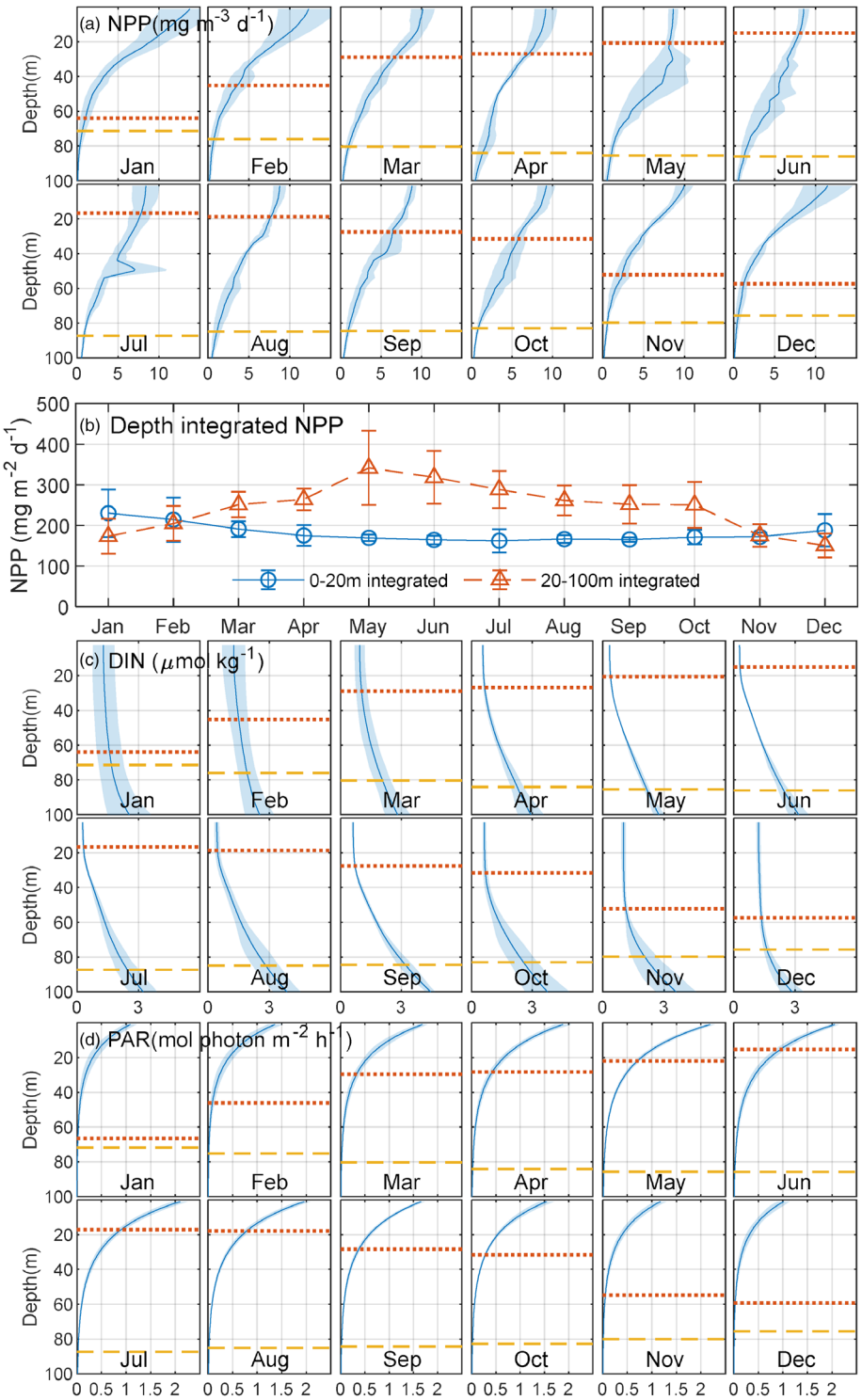


**Fig. 4.** Monthly climatologies of (**a**) net primary production (NPP, mg $m^{-3}$ $day^{-1}$) profiles derived from float measurements; (**b**) monthly climatologies of 0–20 m and 20–100 m integrated NPP (mg $m^{-2}$ $day^{-1}$) derived from float data; (**c**) modeled DIN (nitrate + ammonium) concentration (μmol $kg^{-1}$) from Gomez et al. (2018); and (**d**) photosynthetically active radiation (PAR; mol photon $m^{-2}$ $h^{-1}$). For panels (**a**), (**c**), and (**d**), the red dotted line and yellow dash line indicate the mixed layer depth (MLD) and euphotic depth ($Z_{1\%}$, the depth where the PAR value equals to 1% of surface PAR), and the error bars and shadings indicate the 50% quantile of monthly mean values.

integrated NPP in the 0–20 m layer was higher (Fig. 4b). This pattern indicates that for the open-ocean GoM: (1) NPP in the surface layer (0–20 m) is mostly controlled by nutrient supply; (2) there is no nutrient limitation in the deeper layer (20–100 m), and the carbon production in this layer is mainly controlled by seasonal changes in light level; (3) for most of the year the deeper layer has larger contribution to the total (0–100 m) NPP; (4) in January and February the surface layer contributes more to the total NPP than the deeper 20–100 m layer, due to the enhanced surface nutrient supply from deep mixing and the low light level in the deeper layer.

It should be noted that elevated NPP was observed in mid-depth (~ 50 m) in July (Fig. 4a), together with the elevated Chl and BBP at the same depth (Fig. S3). This mid-depth NPP peak is most likely due to enhanced nutrient supply at this depth. Since the MLD was still shallow it is more likely that the extra nutrient supply was from lateral transport, rather than from vertical mixing. Possible processes that could generate such lateral nutrient transport include the extended Mississippi River plume (Gomez et al. 2018), and mesoscale activities like Loop Current eddies (Damien et al. 2021). However, the climatological DIN profiles from model outputs (Fig. 4c) could not reveal the increased mid-depth nitrate supply. Alternatively, such high NPP signal at mid-depth could also be a result of the lateral transport of organic matter (Kelly et al. 2021).

## Conclusion

In this work, we first evaluated the bio-optical data (Chl and bbp) from the 2012–2015 BOEM float deployments (without concurrent shipboard field calibration) against the satellite remote sensing products. The results showed that the float-measured surface Chl had a good linear relationship with the satellite product, which can be used to adjust the depth-resolved float Chl data. Meanwhile, the float-measured surface bbp had the same magnitude as the satellite product, but no significant linear relationship was found. With the adjusted Chl and unadjusted bbp, for the first time we obtained year-round in situ estimates of depth-resolved NPP in the historically understudied open-ocean GoM. Although there might be some uncertainties in the absolute NPP values due to the lack of shipboard field calibration of Argo data and the bio-optical model parameterization, this year-round depth-resolved NPP dataset provided us a useful tool to study the seasonal and vertical distributions of NPP in this region. The results showed higher surface NPP in the winter due to the increased surface nitrate supply from winter deep mixing. More importantly, the depth-resolved float NPP estimates revealed that the seasonal pattern of depth-integrated (0–100 m) NPP was entirely different from the seasonal pattern of surface NPP, with the highest value in early summer (May). The results indicate that for most of the year the deeper layer (20–100 m) contributes more to the water column NPP than the surface layer (0–20 m), and the major controls of NPP in the deeper layer and surface layer are light level and nutrient supply, respectively.

## References


Behrenfeld, M. J., E. Boss, D. A. Siegel, and D. M. Shea. 2005. Carbon-based ocean productivity and phytoplankton physiology from space. Glob Biogeochem Cycles **19**: GB1006. doi:10.1029/2004GB002299

Boss, E., and others. 2013. The characteristics of particulate absorption, scattering and attenuation coefficients in the surface ocean; contribution of the Tara Oceans expedition. Methods Oceanogr **7**: 52–62. doi:10.1016/j.mio.2013.11.002

Boss, E. B., and N. Haëntjens. 2016, *Primer regarding measurements of chlorophyll fluorescence and the backscattering coefficient with WETLabs FLBB on profiling floats*. Princeton University. doi:10.25607/OBP-50

Damien, P., O. Pasqueron de Fommervault, J. Sheinbaum, J. Jouanno, V. F. Camacho-Ibar, and O. Duteil. 2018. Partitioning of the open waters of the Gulf of Mexico based on the seasonal and interannual variability of chlorophyll concentration. J. Geophys. Res.: Oceans **123**: 2592–2614. doi:10.1002/2017JC013456

Damien, P., J. Sheinbaum, O. Pasqueron de Fommervault, J. Jouanno, L. Linacre, and O. Duteil. 2021. Do loop current eddies stimulate productivity in the Gulf of Mexico? Biogeosciences **18**: 4281–4303. doi:10.5194/bg-18-4281-2021

Davis, J. E. 2017, *The Gulf: The making of an American sea*. Liveright Publishing.

Gomez, F. A., S. K. Lee, Y. Liu, F. J. Hernandez Jr., F. E. Muller-Karger, and J. T. Lamkin. 2018. Seasonal patterns in phytoplankton biomass across the northern and deep Gulf of Mexico: A numerical model study. Biogeosciences **15**: 3561–3576. doi:10.5194/bg-15-3561-2018

Graff, J. R., and others. 2015. Analytical phytoplankton carbon measurements spanning diverse ecosystems. Deep-Sea Res. I: Oceanogr. Res. Pap. **102**: 16–25. doi:10.1016/j.dsr.2015.04.006

Green, R. E., A. S. Bower, and A. Lugo-Fernández. 2014. First autonomous bio-optical profiling float in the Gulf of Mexico reveals dynamic biogeochemistry in deep waters. PloS One **9**: e101658. doi:10.1371/journal.pone.0101658

Hamilton, P., Leidos. 2017. Ocean currents, temperatures, and others measured by drifters and profiling floats for the Lagrangian Approach to Study the Gulf of Mexico's Deep Circulation project 2011-07 to 2015-06 (NCEI Accession 0159562). NOAA National Centers for Environmental Information. Dataset [accessed 2022 Feb 3]. Available from https://www.ncei.noaa.gov/archive/accession/0159562

Kelly, T. B., A. N. Knapp, M. R. Landry, K. E. Selph, T. A. Shropshire, R. K. Thomas, and M. R. Stukel. 2021. Lateral advection supports nitrogen export in the oligotrophic

open-ocean Gulf of Mexico. Nat. Commun. **12**: 3325. doi:10.1038/s41467-021-23678-9

Morel, A., and S. Maritorena. 2001. Bio-optical properties of oceanic waters: A reappraisal. J. Geophys. Res.: Oceans **106**: 7163–7180. doi:10.1029/2000JC000319

Morel, A., Y. Huot, B. Gentili, P. J. Werdell, S. B. Hooker, and B. A. Franz. 2007. Examining the consistency of products derived from various ocean color sensors in open ocean (Case 1) waters in the perspective of a multi-sensor approach. Remote Sens. Environ. **111**: 69–88. doi:10.1016/j.rse.2007.03.012

Muller-Karger, F. E., and others. 2015. Natural variability of surface oceanographic conditions in the offshore Gulf of Mexico. Prog. Oceanogr. **134**: 54–76. doi:10.1016/j.pocean.2014.12.007

Pasqueron de Fommervault, O., P. Perez-Brunius, P. Damien, V. F. Camacho-Ibar, and J. Sheinbaum. 2017. Temporal variability of chlorophyll distribution in the Gulf of Mexico: Bio-optical data from profiling floats. Biogeosciences **14**: 5647–5662. doi:10.5194/bg-14-5647-2017

Selph, E., K. Swalethorp, M. R. Stukel, T. B. Kelly, A. N. Knapp, K. Fleming, T. Hernandez, and M. R. Landry. 2021. Phytoplankton community composition and biomass in the oligotrophic Gulf of Mexico. J. Plankton Res. **43**: fbab006. doi:10.1093/plankt/fbab006

Stukel, M. R., T. B. Kelly, M. R. Landry, K. E. Selph, and R. Swalethorp. 2021. Sinking carbon, nitrogen, and pigment flux within and beneath the euphotic zone in the oligotrophic, open-ocean Gulf of Mexico. J. Plankton Res. **43**: fbab001. doi:10.1093/plankt/fbab001

Westberry, T., M. J. Behrenfeld, D. A. Siegel, and E. Boss. 2008. Carbon-based primary productivity modeling with vertically resolved photoacclimation. Glob. Biogeochem. Cycles **22**: GB2024. doi:10.1029/2007GB003078

Yang, B., J. Fox, M. J. Behrenfeld, E. S. Boss, N. Haëntjens, K. H. Halsey, S. R. Emerson, and S. C. Doney. 2021. In situ estimates of net primary production in the western North Atlantic with float profiling floats. J. Geophys. Res.: Biogeosci. **126**: e2020JG006116. doi:10.1029/2020JG006116

Yingling, N., T. B. Kelly, T. A. Shropshire, M. R. Landry, K. E. Selph, A. N. Knapp, S. A. Kranz, and M. R. Stukel. 2021. Taxon-specific phytoplankton growth, nutrient utilization, and light limitation in the oligotrophic Gulf of Mexico. J. Plankton Res. **43**: fbab028. doi:10.1093/plankt/fbab028

Zhao, Y., and A. Quigg. 2015. Study of photosynthetic productivity in the northern Gulf of Mexico: Importance of diel cycles and light penetration. Cont. Shelf Res. **102**: 33–46. doi:10.1016/j.csr.2015.04.014

## Acknowledgments

BY was partially supported by NOAA's Atlantic Oceanographic and Meteorological Laboratory and by the Cooperative Institute for Marine and Atmospheric Studies (CIMAS), a cooperative institute of the University of Miami and NOAA (cooperative agreement NA20OAR4320472).

*Submitted 01 October 2021*
*Revised 24 April 2022*
*Accepted 01 July 2022*